©SNAK, 2015

Int. J. Nav. Archit. Ocean Eng. (2015) 7:655~669
http://dx.doi.org/10.1515/ijnaoe-2015-0046
pISSN: 2092-6782, eISSN: 2092-6790

The overall motion sickness incidence applied to catamarans

Vincenzo Piscopo and Antonio Scamardella

Department of Sciences and Technology, The University of Naples Parthenope, Naples, Italy

Received 15 October 2014; Revised 9 January 2015; Accepted 24 April 2015

ABSTRACT: *The Overall Motion Sickness Incidence is applied to the hull form optimization of a wave piercing high-speed catamaran vessel. Parametric hull modelling is applied to generate two families of derived hull forms, the former varying the prismatic coefficient and the position of longitudinal centre of buoyancy, the latter instead the demi-hull separation. Several heading angles are analysed in a seaway, considering all combinations of significant wave height and zero-crossing period under two operating scenarios. The optimum hull is generated and vertical accelerations at some critical points on main deck are compared with the parent ones. Finally a comparative analysis with the results obtained for a similarly sized monohull passenger ship is carried out, in order to quantify, by the OMSI, the relative goodness in terms of wellness onboard of monohulls and catamarans, as a function of sea states and operating scenarios.*

KEY WORDS: Overall motion sickness incidence; Catamarans; Hull form optimization.

INTRODUCTION

During the last decade the high-speed waterborne transportation became more and more important, together with the growing interest in developing safer and more comfortable fast ships, capable of being competitive for both domestic, cross-strait and international passenger ferry markets (Fang and Chan, 2007). In this respect, to increase passenger ships' seakeeping performances, designers proposed a wide variety of arrangements, ranging from classical mono-hulls to multi-hulls, mainly with catamaran or SWATH configuration. From this point of view, it is well known that mono-hulls show slower wave induced vertical accelerations (Marón and Kapsenberg, 2014), compared to similarly sized catamarans, especially in moderate and rough sea conditions (Bouscasse et al., 2013), while multi-hulls, catamarans among others, seem to be the most attractive solution in calm and slight seas, thanks to larger deck areas and good transverse stability.

Following the first hydrodynamic experiences on multi-hulls carried out by Everest (1968), many researchers, Insel and Molland (1992), Molland et al. (1995) and Muller-Graf et al. (2002) among others, performed both theoretical and experimental studies, devoted to the assessment of resistance performances of catamarans, paying attention to both demi-hull forms, dimensions and transverse separation. Around the same time the initial pioneering works, devoted to seakeeping analysis of catamarans, were carried out by Kogan (1971), Wahab et al. (1971), Belenky et al. (1979) and subsequently were followed by a variety of theoretical and experimental studies, carried out by many researchers, Faltinsen et al. (1991) among others. In this respect, the improvement of comfort level onboard passenger ships, and the consequent reduction of motion sickness incidence, have been always considered the most important design factors, especially for high-speed vessels (Campana et al., 2009; Diez

Corresponding author: *Vincenzo Piscopo,* e-mail: *vincenzo.piscopo@uniparthenope.it*

and Peri, 2010). The initial studies regarding the motion effects on humans, sponsored by the US Navy in the early 1970's, were carried out by O'Hanlon and McCauley (1974), who conducted a series of experiments on over 500 subjects, exposed to the effects of various combinations of motion frequencies and magnitudes up to two hours, finding that the main sickness cause is the vertical component of the motion. After the development of the first mathematical model by O'Hanlon and McCauley (1974), namely the Motion Sickness Incidence, Lawther and Griffin (1987; 1988) carried out similar studies on car ferries operating in the English Channel and analysed the consequent sickness among passengers. They obtained similar results, in the correlation between MSI and vertical acceleration, but they also found that both roll and pitch motions, even if not provoking sickness in themselves, when combined with heave, may produce more seasickness than predicted by classical models (Wertheim et al., 1998).

As is well known, all motion sickness indices are highly site dependent, as ship vertical acceleration on main deck varies along the ship length and breadth, depending on the heading angle between the vessel route and the prevailing sea direction (Sariöz and Sariöz, 2005; 2006). In this respect, to estimate more reliably the sickness incidence onboard passenger ships, the Overall Motion Sickness Incidence OMSI proposed by Scamardella and Piscopo (2014a), may fulfil this lack and furnish more reliable values of the comfort level onboard passenger ships. In this paper the OMSI is chosen as a parameter to estimate the seakeeping qualities of a high-speed catamaran, varying both demi-hull separation and hull forms. Starting from a wave piercing high-speed catamaran, assumed as a parent hull, a parametric study (Cakici and Aydin, 2014) is carried out, systematically varying both the demi-hull separation and the hull prismatic coefficient. Various heading angles are analysed, under all statistically relevant combinations of significant wave height and zero-crossing period for Mediterranean Sea region, in order to obtain the most reliable value of the above mentioned index. Finally, the obtained results are compared with those ones presented by Scamardella and Piscopo (2014a), for a similarly sized mono-hull at the same speed, to highlight the different behaviour between mono and multi-hulls in terms of comfort levels onboard, as a function of both significant wave height and zero-crossing period.

MOTION SICKNESS EVALUATION

The overall motion sickness incidence

The main parameter to estimate the passenger comfort onboard is the ship vertical acceleration, combined with both roll and pitch motions. The Motion Sickness Incidence (MSI) is defined as the percentage of passengers who vomit after 2 hours of exposure to a certain motion and is given by:

$$MSI = 100\left[0.5 + erf\left(\frac{\log_{10}\left(0.798\sqrt{m_4}/g\right) - \mu_{MSI}}{0.4}\right)\right] \quad (1)$$

where the factor μ_{MSI} is defined as follows, according to O'Hanlon and McCauley (1974):

$$\mu_{MSI} = 0.654 + 3.697\log_{10}\left(\frac{1}{2\pi}\sqrt{\frac{m_4}{m_2}}\right) + 2.320\left[\log_{10}\left(\frac{1}{2\pi}\sqrt{\frac{m_4}{m_2}}\right)\right]^2 \quad (2)$$

or, alternatively, by the following equation proposed by Lloyd (1998):

$$\mu_{MSI} = -0.819 + 2.32\left[\log_{10}\left(\sqrt{\frac{m_4}{m_2}}\right)\right]^2 \quad (3)$$

In Eq. (2) and (3) m_2 and m_4 are the 2^{nd} and 4^{th} spectral moments of the ship vertical motion spectrum $S_z(\omega_e)$, as a function of the encounter frequency ω_e. The MSI was also embodied in 1985 in the ISO Draft International Standard ISO-2631-3:1985, where severe discomfort boundary values of ship vertical accelerations are defined, as a function of motion exposure time and encounter frequency. Subsequently Lawther and Griffin (1987) proposed a new index, namely the Vomiting Incidence (VI), actually embodied in British Standard 6841 (BS 6841, 1987) and ISO Draft International Standard 2631-1:1997 (ISO-2631/1, 1997), proportional to the Motion Sickness Dose Value (MSDV), where the proportional constant is k_m varying in accordance with exposed population characteristics (age, gender):

$$VI = k_m MSDV \tag{4}$$

MSDV depends on both weighted RMS vertical acceleration m_{4W} and exposure time T_d:

$$MSDV = \sqrt{m_{4w} T_d} \tag{5}$$

where m_{4w} is evaluated according to the following formula:

$$m_{4W} = \int_0^\infty \omega_e^4 S_z(\omega_e) G^2(\omega_e) d\omega_e \tag{6}$$

where $G(\omega_e)$ is the frequency weight function, derived by experimental observations and having its maximum in the range 0.111-0.271 *Hz*:

$$G(\omega_e) = \begin{cases} \dfrac{\omega_e}{0.111} & , \omega_e \le 0.111\,Hz \\ 1 & , 0.111 < \omega_e \le 0.271\,Hz \\ \left(\dfrac{0.271}{\omega_e}\right)^{2.85} & , \omega_e > 0.271\,Hz \end{cases} \tag{7}$$

In any case both indices are highly site dependent, as ship vertical acceleration sensibly varies along the vessel length and breadth, as a function of both wave heading and encounter frequency. It follows that an overall index right to account for this variability, may be useful to better estimate the mean comfort level onboard, independently of the assumed position on ship main deck. In this respect, Scamardella and Piscopo (2014a; 2014b) proposed a new index, namely the Overall Motion Sickness Incidence (OMSI), defined as the mean MSI over the main deck area A_{deck}, for any heading angle μ and sea-state, the latter characterized by a certain combination of significant wave height $H_{1/3}$ and zero-crossing period T_z:

$$OMSI_{(H_{1/3},T_z)_j,\mu_k} = \frac{\int_{A_{deck}} MSI_{(H_{1/3},T_z)_j,\mu_k,(x,y,z_{deck})} dA}{A_{deck}} \tag{8}$$

Assuming a uniform distribution of passengers on the main deck, the above formula can be rewritten in a discrete form, mapping the deck area by N_c remote control location points, each one having coordinates $(x,y,z_{deck})_i$.

$$OMSI_{(H_{1/3},T_z)_j,\mu_k} = \frac{1}{N_c}\sum_{i=1}^{N_c} MSI_{(H_{1/3},T_z)_j,\mu_k,(x,y,z_{deck})_i} \tag{9}$$

Finally, denoting by N_s and N_μ the number of analysed sea states and heading angles, each one with a certain probability of occurrence p_j and p_μ respectively, the OMSI finally becomes:

$$OMSI = \frac{1}{N_c}\sum_{j=1}^{N_s} p_j \sum_{k=1}^{N_\mu} p_\mu \sum_{i=1}^{N_c} OMSI_{(H_{1/3},T_z)_j,\mu_k} \tag{10}$$

The above index, also defined for the MII (Scamardella and Piscopo, 2014c) easily allows to compare several variants derived by a parent hull, as well as different vessel types.

Operating scenario and sea spectra

The operating scenario depends on relevant ship mission: in the analysis all heading angles comprised between 45 *deg* and 180 *deg* with 5 *deg* step are considered, disregarding the range comprised between 0-45 *deg*, generally avoided due to possible ship manoeuvring problems. Two different cases are analysed: in the former all heading angles have the same probability of occurrence (see Fig. 1.1), in the latter (see Fig. 1.2) a non-uniform probability density function is assumed, avoiding the heading angles around 90 *deg*.

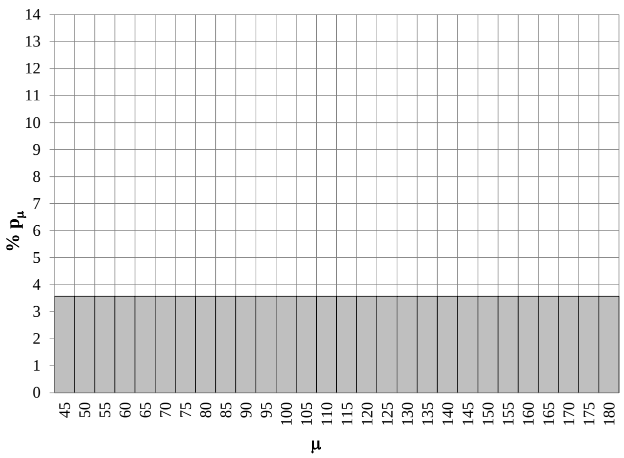

Fig. 1.1 Probability density function vs. heading angle (1st scenario).

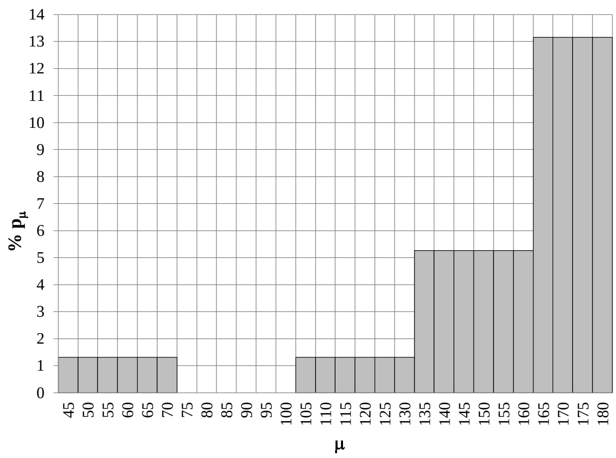

Fig. 1.2 Probability density function vs. heading angle (2nd scenario).

All statistically relevant combinations of significant wave height and zero-crossing period, each one with a certain joint probability of occurrence (see Table 1), have been considered for Mediterranean Sea Region in the summertime period.

Table 1 Scattering diagram for Mediterranean Sea Region – summertime period.

$H_{1/3}$ [*m*]	T_Z [*sec.*]							
	3-4	4-5	5-6	6-7	7-8	8-9	9-10	
0-1	124	182	100	28	5	1	0	**440**
1-2	35	131	133	60	17	3	1	**380**
2-3	6	35	50	30	11	3	1	**136**
3-4	1	7	13	9	4	1	0	**35**
4-5	0	1	3	2	1	0	0	**7**
5-6	0	0	1	1	0	0	0	**2**
	166	**356**	**300**	**130**	**38**	**8**	**2**	**1000**

PARENT AND DERIVED HULL FORMS

Parent hull and remote location points

A wave piercing catamaran (see Table 2), whose demi-hulls are derived by the NPL round bilge systematic series, is chosen as a parent hull. Main data for the ship and hull sections are shown in Table 2 and Fig. 2, respectively. The MSI, as determined by Eq. (1) and (3) have been evaluated, for each sea state and heading angle, at 116 remote location points on the main deck, as shown in Fig. 3. The radius of gyration for pitch of the vessel is 25% L_{OA} and for roll it is 40% B_{OA}, while the roll damping has been determined by relevant heave damping properties. In all cases the non-dimensional ratio $H_{1/3}/L_{WL}$ is comprised between 0.005 and 0.060, as the parent hull waterline length is about 100 *m*, as it will be subsequently shown.

Table 2 Parent hull main dimensions and form parameters.

Displacement	Δ	2288	*t*
Overall length	L_{OA}	96.400	*m*
Overall beam	B_{OA}	45.000	*m*
Draft to Baseline	T	4.000	*m*
Scantling depth	D	15.000	*m*
Waterline length	L_{WL}	91.552	*m*
Waterline beam	B_{WL}	44.944	*m*
Prismatic coefficient	C_P	0.770	
Block coefficient	C_B	0.616	
Midship section coefficient	C_M	0.800	
Waterplane area coefficient	C_{WP}	0.776	
LCB from FP (+ve aft)	LCB	59.00	% L_{WL}
Vertical centre of buoyancy	KB	2.272	*m*
Vertical centre of gravity	KG	12.000	*m*
Demihull spacing	S	40.000	*m*

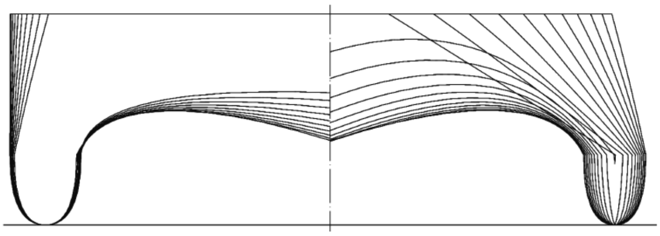

Fig. 2 Parent hull forms.

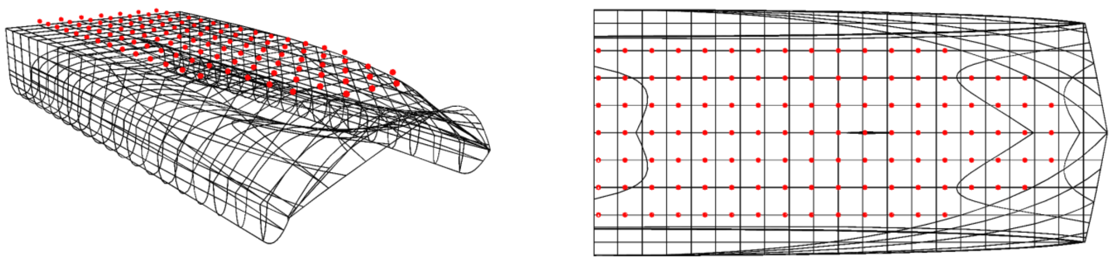

Fig. 3 3D view and horizontal lay-out of the hull with remote location points.

Seakeeping analysis has been carried out at a reference speed of 20 *kn*, corresponding to F_n=0.34, in order to subsequently compare relevant results with those ones obtained by Scamardella and Piscopo (2014a), for a similarly sized monohull. The analysis was performed by a commercial code, suitable for both monohulls and catamarans, based on the linear strip theory model developed by Salvesen et al. (1970). Concerning the computational effort, for each analysed sea-state described by a JONSWAP spectrum, considering 28 equally spaced headings in the range 45-180 *deg*, the computational time is about 10 *min*, which implies that the total time amount for each vessel is about 90 *min*, including the post-processing phase, carried out by a dedicated programme developed in MATLAB MathWorks. It is noticed that horizontal accelerations have not been considered in the evaluation of MSI, as according to the findings of a recent EU project COMPASS (Turan, 2006), the role of horizontal accelerations for the occurrence of MSI is appreciable onboard high speed vessels (F_n>0.50), so confirming the results of some experiments carried out in the past on a standard catamaran, a Deep/V monohull and a wave piercing catamaran. A similar conclusion has also been drawn by Tamura and Arima (2006), while investigating the ride comfort of a high-speed passenger craft.

Derived hull forms

Two different families of derived hulls have been generated, at the same Froude number and displacement. One is derived changing, by a parametric transformation (Kukner and Sariöz, 1995; Grigoropoulos, 2004; 2010; Özüm et al., 2011), both the prismatic coefficient and the longitudinal centre of buoyancy; the other is obtained varying the demi-hull spacing. It is noticed that recent studies on monohulls demonstrated that the vertical motions including absolute vertical acceleration are influenced by vessel main dimensions, length to displacement ratio, longitudinal center of buoyancy, longitudinal center of flotation, waterplane area coefficient and vertical prismatic coefficient with their forward (F) and aft (A) hull portions (Sayli et al., 2007; 2010), so that the present optimization study to lower OMSI can be further explored by considering other design variables of hull form. In Table 3 data for the first group of derived hull forms are shown: the prismatic coefficient is varied in the range 0.74–0.80 with 0.03 step, for three different values of LCB, namely 58, 59 and 60 percent of waterline length from the ship forward perpendicular. In Table 4 data for the second group of derived hull forms are presented: the demi-hull spacing is varied in the range ±5%S for fixed values of longitudinal centre of buoyancy and hull coefficients. In all cases data in bold refer to the parent hull.

Table 3 Alternative hull forms adimensional parameters for fixed demi-hull spacing S=40.00 *m* and C_B=0.616.

	Hull 1- LCB=58%	Hull 0- LCB=58%	Hull 2- LCB=58%
LCB from FP (+ve fwd) % L_{WL}	58%	58%	58%
C_P	---	0.770	0.800
C_M	---	0.800	0.778
C_{WP}	---	0.775	0.797
	Hull 1- LCB=59%	**Hull 0- LCB=59%**	Hull 2- LCB=59%
LCB from FP (+ve fwd) % L_{WL}	59%	**59%**	59%
C_P	0.740	**0.770**	0.800
C_M	0.833	**0.800**	0.778
C_{WP}	0.746	**0.776**	0.799
	Hull 1- LCB=60%	Hull 0- LCB=60%	Hull 2- LCB=60%
LCB from FP (+ve fwd) % L_{WL}	60%	60%	60%
C_P	0.740	0.770	---
C_M	0.833	0.800	---
C_{WP}	0.747	0.777	---

Table 4 Alternative hull forms adimensional parameters for fixed C_B=0.616, C_P=0.770 and LCB=59% L_{WL}.

	Hull 1-S=38.00 *m*	**Hull 0-S=40.00 *m***	Hull 2-S=42.00 *m*
C_B - C_M - C_{WP}	as for parent hull		

SEAKEEPING ANALYSIS

Influence of heading angles and zero-crossing period

It is well known that onboard passengers can occupy good places, generally near the ship centre of gravity, and not so good places (Esteban et al., 2005; Pérez Arribas and López Pineiro, 2007), as vertical accelerations generally increase going to bow or stern, or towards ship sides, depending on heading angles and zero-crossing periods (Scamardella and Piscopo, 2014a; 2014b). The Motion Sickness Incidence significantly varies with heading angles. In Fig. 4 the OMSI is plotted versus heading angles for different values of zero-crossing period and fixed significant wave height. It is interesting to note that the shape of the curve is significantly influenced by the zero-crossing period: while for lower T_z values the maximum occurs at transverse headings, significantly decreasing before and beyond this range, for higher T_z values the curve is almost flat beyond 90 *deg*. These curves are well in accordance with those ones proposed by Fang and Chan (2007) who observed that under a significant wave height of 1.47 *m* and a period of 7 *sec.*, for a wave piercing catamaran MSI values vary with the vessel heading in relation to wave direction, being negligible in stern waves, increasing to bow quartering seas.

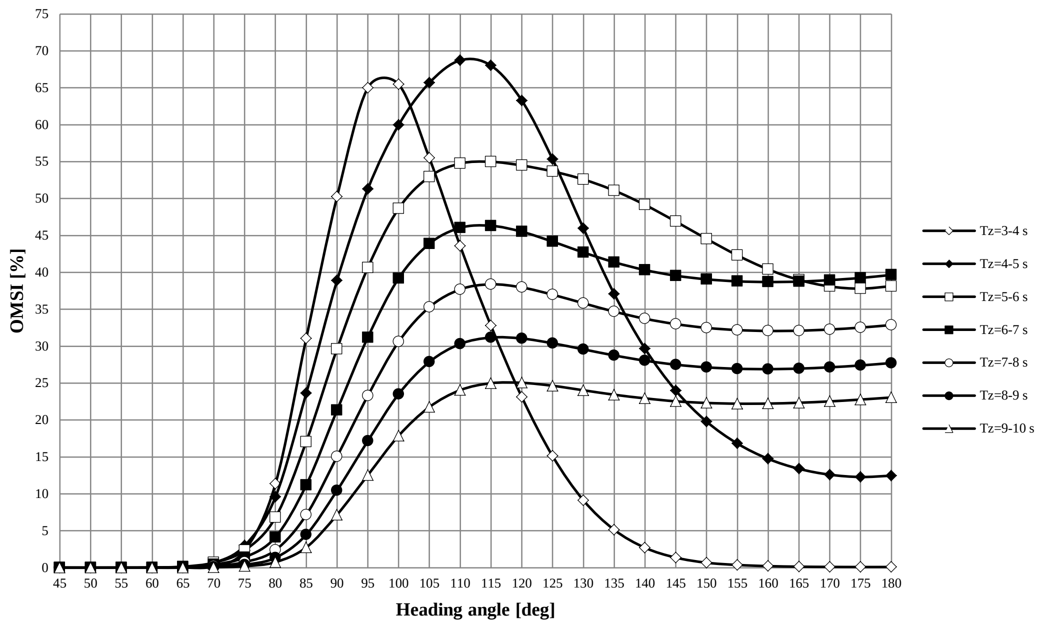

Fig. 4 OMSI distribution versus heading angles for different values of T_z and $H_{1/3}$=2.5 *m*.

In Figs. 5 and 6 OMSI is plotted versus the wave zero-crossing period, for different values of significant wave height, accounting to the operating scenarios of Figs. 1.1 and 1.2, respectively. In both cases it has been found that OMSI is maximum when T_z lies in the range 5–6 *sec.*, significantly decreasing for higher and lower values. In fact, by the dispersion relation (Lewis, 1989), deep water waves with zero-crossing period in the range 5–6 *sec.* have a length of about 47 *m*, so close to the beam and the half length of the ship. Furthermore, even if roll (3.5 *sec.*) and pitch (4.8 *sec.*) natural periods are quite low, due to the high transverse and longitudinal metacentric height of the ship, heave natural period is 5.1 *sec.*, so that resonance occurs and vertical accelerations, as well as OMSI indices, increase. The preliminary analysis clearly shows the only head sea condition is not sufficient to find the optimum hull and several sea-states have to be considered.

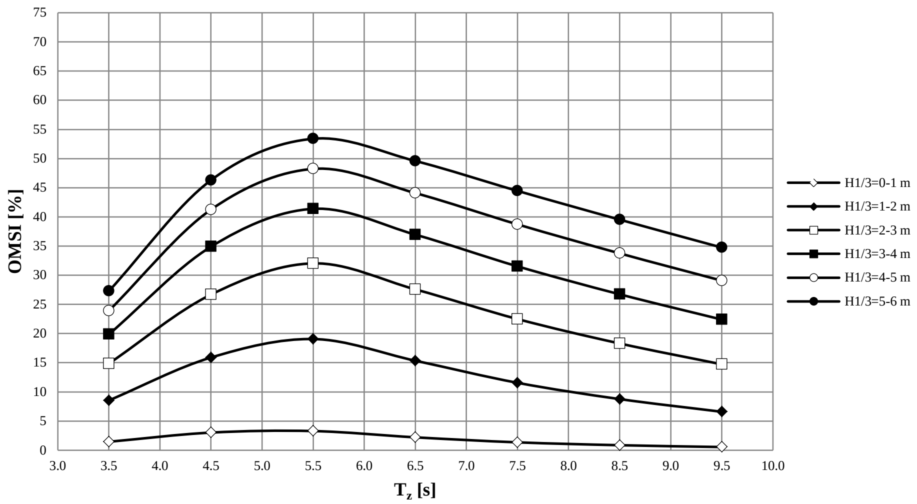

Fig. 5 OMSI distribution versus T_z for different values of significant wave height $H_{1/3}$.

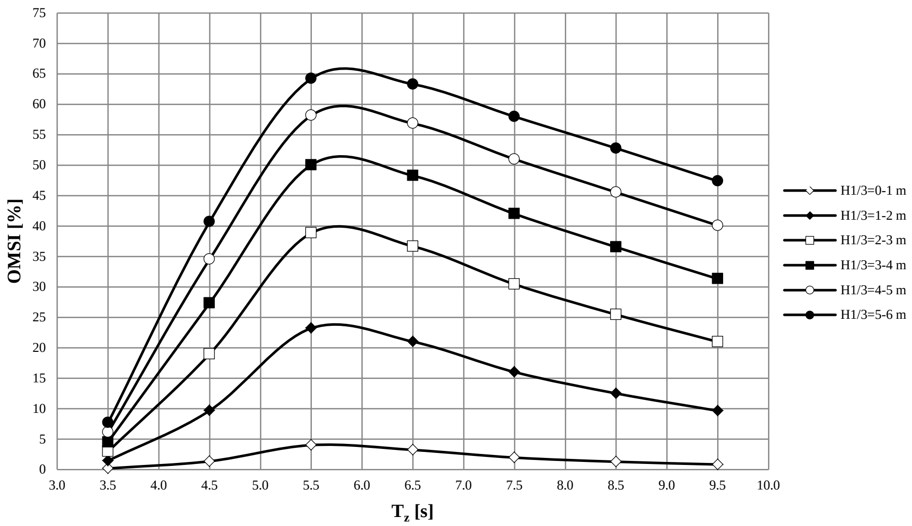

Fig. 6 Weighted OMSI distribution versus T_z for different values of the significant wave height $H_{1/3}$.

Change of C_P, LCB and demi-hull separation

As previously said, in the first operating scenario all heading angles have the same probability of occurrence. Tables 5 and 6 show the OMSI values for both derived hull form groups. Table 7 and 8 show, for the second operating scenario, the same results. In both cases it seems that the optimum hull may be found by shifting the longitudinal centre of buoyancy afterward, by increasing the prismatic coefficient and by decreasing the block and midship section ones, though it is obvious we have to pay attention to both maximum allowable trim and unwanted bare hull resistance increase.

Table 5 OMSI for the first group of alternative hull forms for fixed C_B=0.616.

	Hull 1- LCB=58% C_P=0.740	Hull 0- LCB=58% C_P=0.770	Hull 2- LCB= LCB=58% C_P=0.800
OMSI %	---	11.999	11.815
	Hull 1- LCB=59% C_P=0.740	Hull 0- LCB=59% C_P=0.770	Hull 2- LCB= LCB=59% C_P=0.800
OMSI %	12.922	12.667	12.710
	Hull 1- LCB=60% C_P=0.740	Hull 0- LCB=60% C_P=0.770	Hull 2- LCB= LCB=60% C_P=0.800
OMSI %	13.599	13.510	---

Table 6 OMSI for the second group of alternative hull forms for fixed C_B=0.616, C_P=0.770 and LCB=59% L_{WL}.

	Hull 1-S=38.00 *m*	Hull 0-S=40.00 *m*	Hull 2-S=42.00 *m*
OMSI %	12.768	12.667	12.725

Table 7 Weighted OMSI for the first group of alternative hull forms for fixed C_B=0.616 – Effective heading angle distribution.

	Hull 1- LCB=58% C_P=0.740	Hull 0- LCB=58% C_P=0.770	Hull 2- LCB= LCB=58% C_P=0.800
OMSI %	---	11.817	11.750
	Hull 1- LCB=59% C_P=0.740	Hull 0- LCB=59% C_P=0.770	Hull 2- LCB= LCB=59% C_P=0.800
OMSI %	12.982	12.915	13.301
	Hull 1- LCB=60% C_P=0.740	Hull 0- LCB=60% C_P=0.770	Hull 2- LCB= LCB=60% C_P=0.800
OMSI %	14.069	14.387	---

Table 8 Weighted OMSI for the second group of alternative hull forms for fixed C_B=0.616, C_P=0.770 and LCB=59% L_{WL} – Effective heading angle distribution.

	Hull 1-S=38.00 *m*	Hull 0-S=40.00 *m*	Hull 2-S=42.00 *m*
OMSI %	13.056	12.915	13.045

Optimum hull generation

On further investigation of changing other hull form parameters, it was found that the optimum hull may be generated by shifting the centre of buoyancy towards the center of deck area devoted to passengers, depending on both equilibrium and trim considerations, subsequently increasing as far as possible the prismatic coefficient and decreasing the midship section and waterplane area coefficients. In all cases these variations cannot penalize the bare hull resistance. Table 9 shows main data for the parent and the optimum hulls, while in Fig. 7 optimum hull form is compared with that of the parent. Continuous black and dashed red lines refer to parent and optimum hulls, respectively.

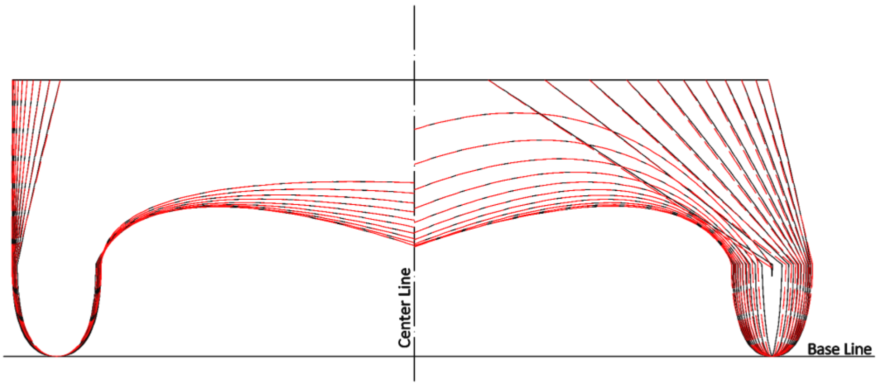

Fig. 7 Parent and optimum hull forms.

Hull forms show some differences. The optimum hull is more slender in the aft body, which implies that the longitudinal centre of buoyancy is shifted about 1%L_{WL} forward. The relevant OMSI is equal to 11.815% with 6.7% reduction with regard to the parent hull value, while for the second scenario it is equal to 11.750% with 9.0% reduction, which implies that slight hull form variations may produce appreciable seakeeping improvements, obviously without altering the bare hull resistance. In Fig. 8 sectional area curves for both parent and optimum hulls are also plotted: redistribution of submerged volume is recognized, with an increase of the fore volume and a consequent decrease of the after one. The adopted reference system has the origin at the midship. Besides, in order to compare the parent and the optimum hulls in terms of vertical accelerations, six remote control points on the ship main deck have been chosen. Table 9 shows the relevant coordinates, respect to the reference system having the origin in correspondence of baseline at the midship.

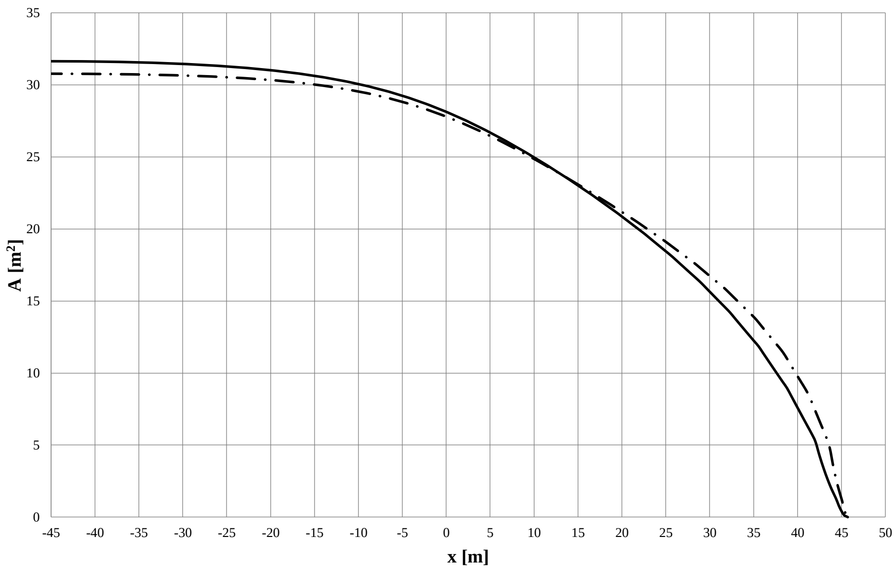

Fig. 8 Sectional area distribution for parent (continuous line) and optimized (pointed-dashed line) hull forms.

Table 9 Parent and optimum hull main dimensions.

		Parent hull	Optimum hull	
Displacement	Δ	2288	2288	*t*
Draft to Baseline	T	4.000	4.000	*m*
Waterline length	L_{WL}	91.552	91.552	*m*
Waterline beam	B_{WL}	44.944	44.944	*m*
Prismatic coefficient	C_P	0.770	0.800	
Block coefficient	C_B	0.616	0.617	
Midship section coefficient	C_M	0.800	0.778	
Waterplane area coefficient	C_{WP}	0.776	0.797	
LCB from FP (+ve aft)	LCB	59.00	58.00	% L_{WL}
Overall Motion Sickness Incidence (1st scenario)	OMSI	12.667	11.815	%
Overall Motion Sickness Incidence (2nd scenario)	OMSI	12.915	11.750	%

The first three remote location points are located at centreline, while the other three are 15 *m* sideward. Figs. 9(a)-9(d) show the R.M.S. of vertical acceleration at remote control points 1-2-3 as function of the encounter frequency f_e, in the range between 0 *Hz* and 1 *Hz*, with 0.1 *Hz* step. Similarly in Figs. 10(a)-10(d) the similar results are shown for the remote control points 4-5-6.

In all cases acceleration curves refer to a seaway described by a JONSWAP Spectrum with a significant wave height $H_{1/3}$=1.0 *m* and a zero-crossing period T_z=6.5 *sec*. The obtained results clearly show that the parent and the optimum hull acceleration component due to roll motion is substantially unchanged, while the heave and pitch motion components are substantially lower for the optimum hull, especially in the heading range from beam to head seas. A slight increment is found only at quartering sea, but it doesn't penalize the OMSI, due to the low values of relevant accelerations. These clearly show the difficulty in estimating the real improvements of comfort onboard by only comparing acceleration values at the same critical points. Therefore an overall index, such as the OMSI, could be more suitable for this purpose and, eventually, for comparing similarly sized vessels with different hull configurations, as it will be subsequently shown.

Table 10 Remote location points where vertical accelerations have been evaluated.

Description	Units	1	2	3	4	5	6
Longitudinal position (+ve fwd)	*m*	-45.0	0.0	40.0	-45.0	0.0	20.0
Offset from centreline	*m*	0.0	0.0	0.0	15.0	15.0	15.0
Vertical position	*m*	16.0	16.0	16.0	16.0	16.0	16.0

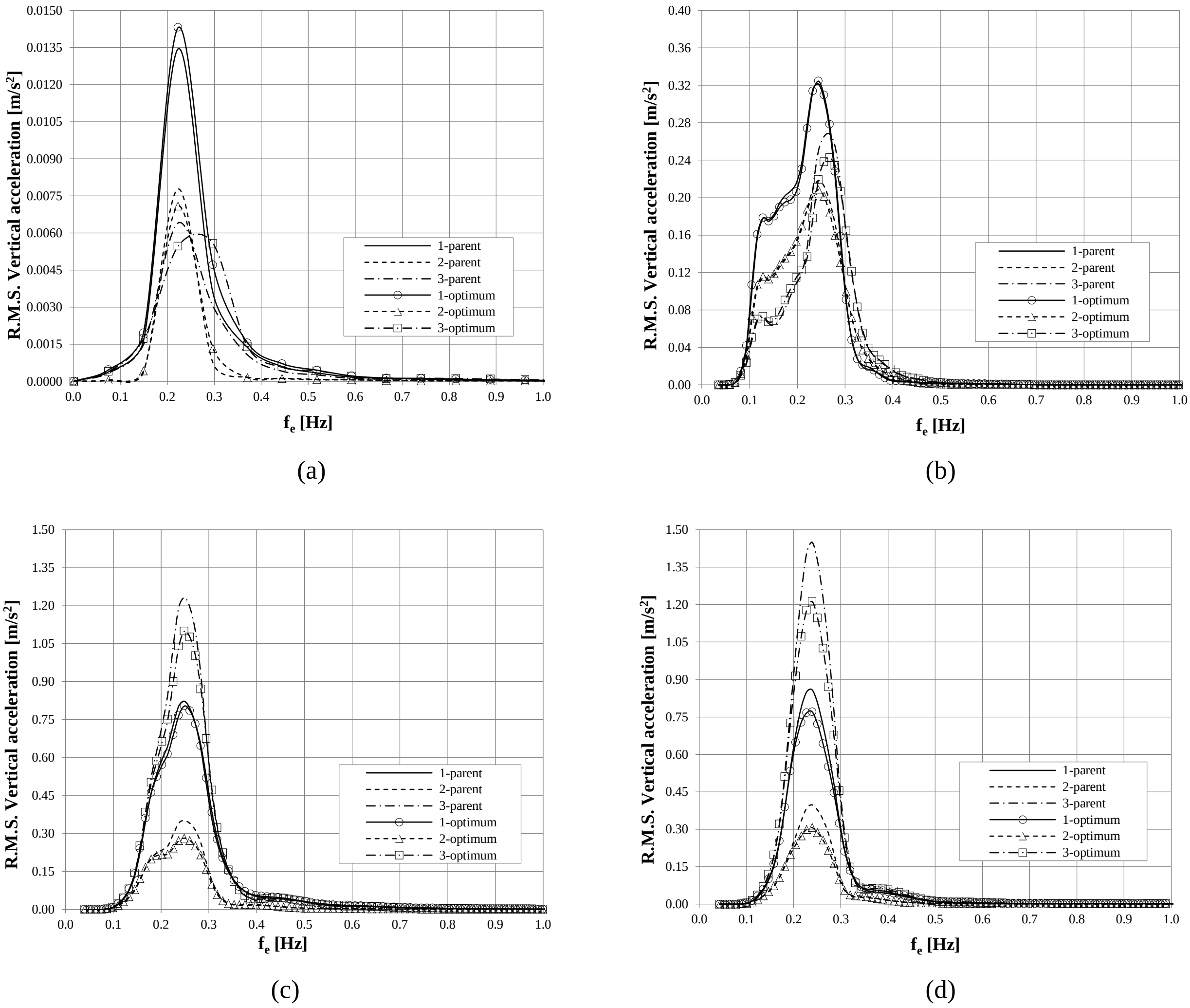

Fig. 9 (a) Vertical accelerations (1-2-3) – Heading angle=45 *deg* (b) Vertical accelerations (1-2-3) – Heading angle =90 *deg* (c) Vertical accelerations (1-2-3) – Heading angle =135 *deg* (d) Vertical accelerations (1-2-3) – Heading angle =180 *deg*.

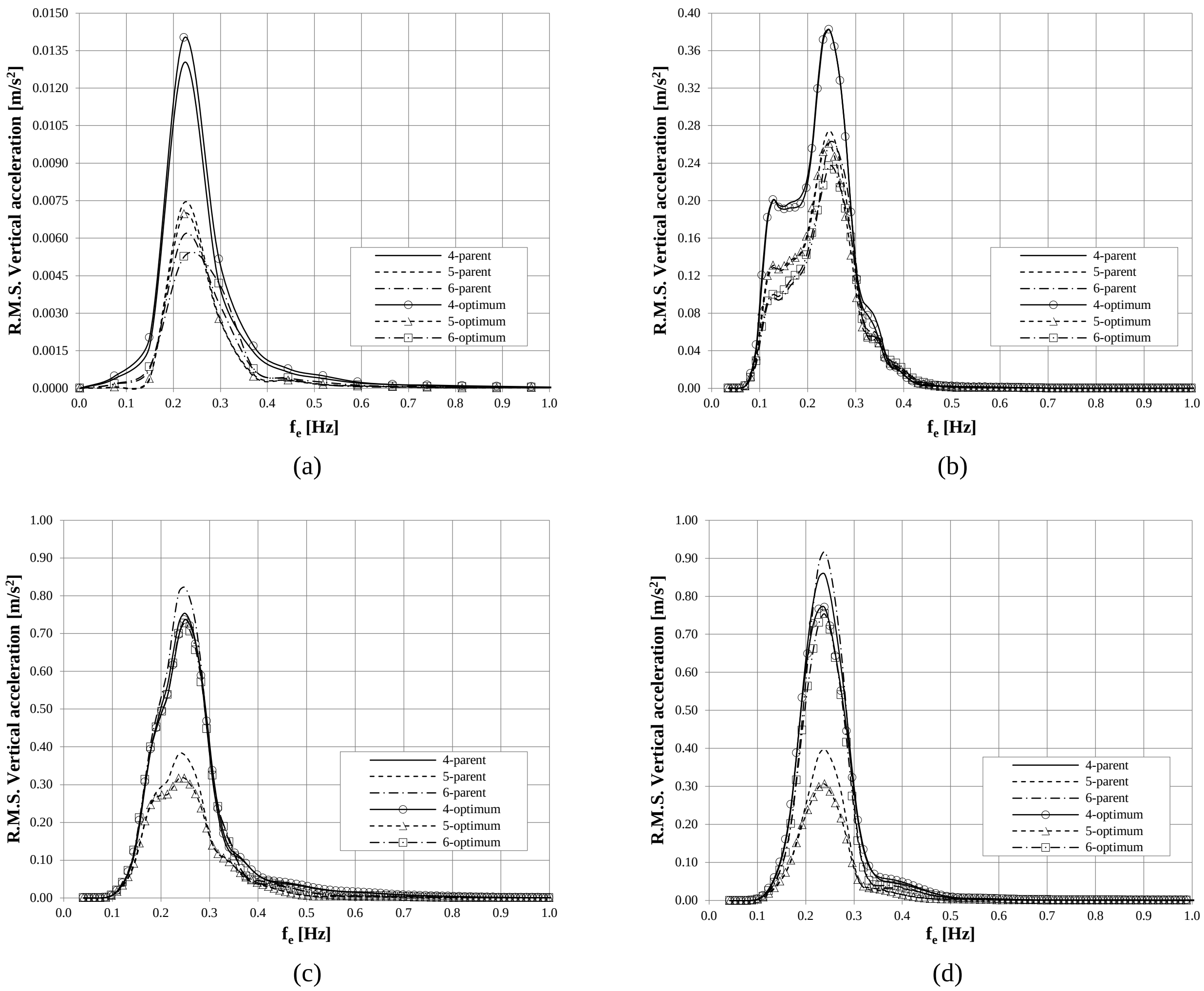

Fig. 10 (a) Vertical accelerations (4-5-6) – Heading angle=45 *deg* (b) Vertical accelerations (4-5-6) – Heading angle =90 *deg* (c) Vertical accelerations (4-5-6) – Heading angle =135 *deg* (d) Vertical accelerations (4-5-6) – Heading angle =180 *deg*.

COMPARISON BETWEEN MONOHULLS AND CATAMARANS

It is well known that monohulls behave better in rough water than similarly sized catamarans at the same speed (Atlar et al., 2013). In Scamardella and Piscopo (2014a) both seakeeping analysis and optimization of a passenger ship with monohull configuration were performed and the OMSI index was determined as a function of significant wave height and zero-crossing period. In Fig. 11 a comparison between similarly sized passenger ships with monohull and catamaran configurations is carried out. The OMSI is plotted versus significant wave height: curves with full and empty markers refer to catamaran and monohull configuration, respectively; the former operating scenario (see Fig. 1.1) is represented by a continuous line, while the latter (see Fig. 1.2) by a dashed line. The obtained results not only confirm that monohulls offer superior seakeeping performances than catamarans, but also suggest further considerations about the influence of sea state and operating scenario on passenger ships' comfort level. In this respect, if all heading angles are assumed to have the same probability of occurrence, the catamaran OMSI is on the average 1.5 times higher than the monohull; while in the second operating scenario it is about 3.0 times higher. Furthermore, the percentage difference between relevant values decreases when the significant wave height increases, too. In terms of overall values the final OMSI index is equal to 12.667% and 8.479% for catamaran and monohull respectively, for the first operating scenario; for the second they are 12.915% and 4.255%, respectively. It is noted that the difference is greater for the second scenario due to the assumed heading angle probability density function (2nd operating scenario), where transverse headings are totally avoided. In this respect, the OMSI distribution vs. heading angles for monohulls shows a distinct peak at transverse headings (Scamardella and Piscopo, 2014a), decaying before and beyond this range. On the contrary, the same distribution for catamarans shows a maximum ranging from 90 *deg* to 115 *deg*, as function of wave zero-crossing period, being almost constant up to head seas. It follows that the final OMSI index significantly decreases for monohulls, if transverse headings are avoided, while the same result cannot be achieved for catamarans.

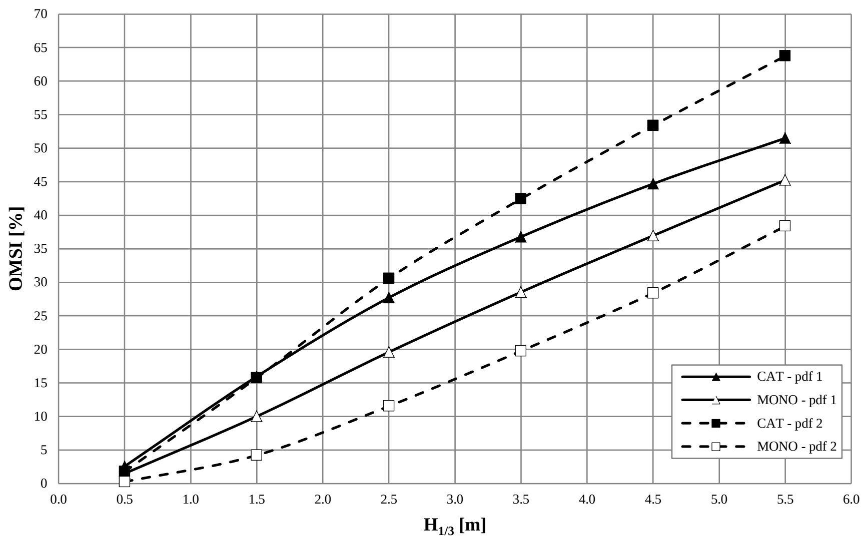

Fig. 11 OMSI distribution versus significant wave height for catamaran and monohull.

CONCLUSIONS

The Overall Motion Sickness Incidence was chosen as a parameter to be minimized in the optimization procedure of a passenger ship with a catamaran configuration, in order to improve both wellness and comfort onboard. Despite of classical procedures, mainly based on finding the optimum hull with the minimum combined vertical acceleration due to heave and pitch motions, in some chosen control location points and in regular head waves, all heading angles have been analysed in a seaway, accounting for all relevant combinations of significant wave height and zero-crossing period for the Mediterranean Sea in summertime period. Two operating scenarios have been analysed, assuming in the former that all heading angles have the same probability of occurrence, while in the latter a specific probability density function, mainly avoiding beam sea angles.

A wave piercing high-speed catamaran was chosen as a test case and two alternative hull forms have been generated, by varying both prismatic coefficient and longitudinal centre of buoyancy position and the demi-hull separation. It was found out that the demi-hull separation doesn't significantly influence the OMSI index, but appreciable improvements of comfort onboard are possible by increasing the prismatic coefficient and shifting the longitudinal centre of buoyancy towards the centre of deck area, devoted to passengers. Furthermore the analysis clearly shows that all of heading angles, sea states and operating scenarios significantly influence the overall hull performances and are important for a more refined optimization procedure. Finally the suitability of the OMSI index, that could also be extended to MII (Scamardella and Piscopo, 2014c), has also been shown by comparing relevant results obtained for a similarly sized monohull, finding not only that monohulls behave better than catamarans in rough water, as it is well known, but also that how big is this difference. It follows that the OMSI of catamarans is up to 3 times higher than that of a similarly sized monohull at the same speed, depending on both sea state and operating scenario. The procedure could be extended to other hull forms and ship types, assuring, in any case, the availability of a simple and effective comparison of different vessels, by means of a unique overall index of comfort level onboard.

ACKNOWLEDGEMENTS

The work has been financed by the Department of Science and Technology of the University of Naples "Parthenope", under the Research Project PROGETTO INSIST "Innovazione Tecnologica nei Sistemi di Trasporto" POR Campania FSE 2007/ 2013 CUP B25B09000040007 - Research Stream: "Ottimizzazione della tenuta al mare di mezzi navali ai fini del miglioramento del Comfort e della Sicurezza dei passeggeri e del personale imbarcato".

REFERENCES

Atlar, M., Seo, K., Sampson, R. and Danisman, D.B., 2013. Anti-slamming bulbous bow and tunnel stern applications on a novel Deep-V catamaran for improved performance. *International Journal of Naval Architecture and Ocean Engineering*, 5(2), pp.302-312.

Belenky, L.M. et al., 1979. *Catamarans experiment*. Leningrad: Shipbuilding, pp.1-132.

Bouscasse, B., Broglia, R. and Stern, F., 2013. Experimental investigation of a fast catamaran in head waves. *Ocean Engineering*, 72, pp.318-330.

BS 6841, 1987. *Guide to measurement and evaluation of human exposure to whole-body mechanical vibration and repeated shock*. London: British Standard Institution.

Cakici, F. and Aydin, M., 2014. Effects of hull form parameters on seakeeping for YTU gulet series with cruiser stern. *International Journal of Naval Architecture and Ocean Engineering*, 6(3), pp.700-714.

Campana, E.F., Liuzzi, G., Lucidi, S., Peri, D., Piccialli, V. and Pinto, A., 2009. New global optimization methods for ship design problems. *Optimization Engineering*, 10(4), pp.533-555.

Diez, M. and Peri, D., 2010. Robust optimization for ship conceptual design. *Ocean Engineering*, 37(11-12), pp.966-977.

Esteban, S., Giron-Sierra, J.M., De-Andres Toro, B., De La Cruz, J.M. and Riola, J.M., 2005. Fast ships models for seakeeping improvement studies using flaps and T-Foil. *Mathematical and Computer Modeling*, 41(1), pp.1-24.

Everest, J.T., 1968. *Some research on the hydrodynamics of catamarans and multi-hulled vessels in calm water. ship Report 128*. London: National Physical Laboratory(NPL).

Faltinsen, O.M., Helmers, J.B., Minsaas, K.J. and Zhao, R., 1991. Speed loss and operability of catamarans and SES in a seaway. In: Holden, K.O., Faltinsen, O.M., Moan, T. (Eds.). *Proceedings of the First on Fast Sea Transportation FAST'91 Trondheim June, 1991*, pp.709-725.

Fang, C.C. and Chan, H.S., 2007. An investigation on the vertical motion sickness characteristics of a high-speed catamaran ferry. *Ocean Engineering*, 34(14-15), pp.1909-1917.

Grigoropoulos, G.J., 2004. Hull form optimization for hydrodynamic performance. *Marine Technology and SNAME News*, 41(4), pp.167-182.

Grigoropoulos, G.J., 2010. Hull form optimization in calm and rough water. *Computer-Aided Design*, 42(11), pp.977-984.

Insel, M. and Molland, A., 1992. Investigation into the resistance components of high speed displacement catamarans. *Transactions of the Royal Institution of Naval Architects*, 134, pp.1-20.

ISO-2631/1, 1997. *Evaluation of human exposure to whole-body vibration. Part 1*. Geneva: The International Standard Organization.

Kogan, E.M., 1971. To the calculation of main part of disturbing forces for oscillating catamaran in liquid of finite depth. *Proceedings of Nikolaev Shipbuilding Institute of adm. S. O. Makarov - Ships Theory*, 44, pp.42-45.

Kukner, A. and Sariöz, K., 1995. High speed hull form optimisation for seakeeping. *Advances in Engineering Software*, 22(3), pp.179-189.

Lawther, A. and Griffin, M.J., 1987. Prediction of the incidence of motion frequency and duration of vertical oscillation. *The Journal of the Acoustical Society of America*, 82, pp.957-966.

Lawther, A. and Griffin, M.J., 1988. A survey of the occurrence of motion sickness amongst passengers at sea. Characteristics of vessels at sea. *Aviation, Space and Environmental Medicine*, 56, pp.399-406.

Lewis, E.V., 1989. *Principles of naval architecture second revision – volume III motions in waves and controllability*. Jersey City: The Society of Naval Architects and Marine Engineers.

Lloyd, A.R.J.M., 1998. *Seakeeping ship behaviour in rough water*. Hampshire: A.R.J.M. Llyod.

Marón, A. and Kapsenberg, G., 2014. Design of a ship model for hydro-elastic experiments in waves. *International Journal of Naval Architecture and Ocean Engineering*, 6(4), pp.1130-1147.

Molland, A.F., Wellicome, J.F. and Couser, P.R., 1995. *Experimental measurements of the seakeeping characteristics of fast displacement catamarans in long-crested head-seas. Ship science report No. 89*. Southampton: University of Southampton.

Muller-Graf, B., Radojcic, D. and Simic, A., 2002. Resistance and propulsion characteristics of the VWS hard chine catamaran hull series '89. *SNAME Transactions*, 110, pp.1-29.

O'Hanlon, J.F. and McCauley, M.E., 1974. Motion sickness as a function of the frequency and acceleration of vertical sinusoidal motion. *Aerospace Medicine*, 45(4), pp.366-369.

Özüm, S., Şener, B., Yilmaz, H., 2011. A parametric study on seakeeping assessment of fast ships in conceptual design stage. *Ocean Engineering*, 38(13), pp.1439-1447.

Pérez Arribas, F.L. and López Pineiro, 2007. Seasickness prediction in passenger ships at the design stage. *Ocean Engineering*, 34(14-15), pp.2086-2092.

Sayli, A., Alkan, A.D., Nabergoj, R. and Uysal, A.O., 2007. Seakeeping assessment of fishing vessels in conceptual design stage. *Ocean Engineering*, 34(5-6), pp.724-738.

Sayli, A., Alkan, A.D. and Ganiler, O., 2010. Nonlinear meta-models for conceptual seakeeping design of fishing vessels. *Ocean Engineering*, 37(8-9), pp.730-741.

Sariöz, K. and Sariöz, E., 2005. Habitability assessment of passenger vessels based on ISO criteria. *Marine Technology*, 42(1), pp.43-51.

Sariöz, K. and Sariöz, E., 2006. Practical seakeeping performance measures for high speed displacement vessels. *Naval Engineers Journal*, 118(4), pp.23-36.

Salvesen, N., Tuck, O.E., Faltinsen, O., 1970. Ship motions and sea loads. *Transactions, Society of Naval Architects and Marine Engineers*, 78, pp. 250-287.

Scamardella, A. and Piscopo, V., 2014a. Passenger ship seakeeping optimization by the overall motion sickness incidence. *Ocean Engineering*, 76, pp.86-97.

Scamardella, A. and Piscopo, V., 2014b. Twin-deck Ro-ro/Pax ship seakeeping optimization by the motion sickness incidence. *15th International Congress of the International Maritime Association of the Mediterranean*, 1, pp.109-117.

Scamardella, A. and Piscopo, V., 2014c. The overall motion induced interruptions in seakeeping optimization analysis. *15th International Congress of the International Maritime Association of the Mediterranean*, 1, pp.119-126.

Tamura, Y. and Arima, M., 2006. Measurement and analysis of ship motion of a high-speed passenger craft. *Proceedings of the Sixteenth International Offshore and Polar Engineering Conference*, San Francisco, California, USA May-June, pp.514-519.

Turan, O., 2006. *A rational approach for reduction of motion sickness and improvement of passenger comfort and safety in sea transportation (COMPASS). COMPASS Project Technical Report*. Glasgow: Universities of Glasgow and Strathclyde.

Wahab, R., Pritchett, C. and Ruth, L.C., 1971. On the Behavior of the ASR catamaran in waves. *Marine Technology*, 8, pp.334-360.

Wertheim, A.H., Bos, J.E. and Bles, W., 1998. Contributions of roll and pitch to sea sickness. *Brain Research Bulletin*, 47(3), pp.517-524.